

Supplementary Information for

The Reactions of Terphenyl Substituted Digallene $\text{Ar}^{i\text{Pr}_4}\text{GaGaAr}^{i\text{Pr}_4}$ ($\text{Ar}^{i\text{Pr}_4} = \text{C}_6\text{H}_3\text{-2,6-(C}_6\text{H}_3\text{-2,6-}i\text{Pr}_2)_2$) with Transition Metal Carbonyls and Theoretical Investigation of the Mechanism of Addition

Madison L. McCrea-Hendrick,¹ Christine A. Caputo,¹ Christopher J. Roberts,² James C. Fettinger,¹
Heikki M. Tuononen,^{2*} Philip P. Power^{1*}

¹ Department of Chemistry, The University of California Davis, 1 Shields Ave., Davis, CA, USA.
Tel: 1-530-752-8900; Fax: 1-530-732-8995; E-mail: pppower@ucdavis.edu.

² University of Jyväskylä, Department of Chemistry, Nanoscience Center, P.O. Box 35, FI-40014
University of Jyväskylä, Finland. Tel: 358-40-805-3713; Fax: 358-14-260-2501; E-mail:
heikki.m.tuononen@jyu.fi.

Table of Contents	Page
1. Selected X-ray Crystallographic Data for 1–5 -----	S2
2. Spectroscopic Data for Compound 1 -----	S3-S5
3. Spectroscopic Data for Compound 2 -----	S5-S7
4. Spectroscopic Data for Compound 3 -----	S8-S9
5. Spectroscopic Data for Compound 4 -----	S10-S11
6. Spectroscopic Data for Compound 5 -----	S12-S13

Table S1. Selected X-ray Crystallographic Data for **1–5**.

Compound	1	2	3	4	5
Empirical formula	C ₆₄ H ₇₄ Ga ₂ O ₄ Cr	C ₆₄ H ₇₄ Ga ₂ O ₄ Mo	C ₆₄ H ₇₄ Ga ₂ O ₄ W	C ₃₅ H ₃₇ GaMoO ₅	C ₃₇ H ₃₇ Co ₂ GaO ₇
Formula weight , gmol ⁻¹	1098.67	1142.61	1230.52	703.30	781.25
T (K) / l(Å)	90(2) / 0.71073	90(2) / 0.71073	90(2) / 1.54178	90(2) / 0.71073	87(2) / 0.71073
Crystal system	monoclinic	monoclinic	monoclinic	Monoclinic	triclinic
Space group / Z	C2/c / 8	C2/c / 8	C2/c / 8	P2 ₁ /c / 8	P ₁ / 2
a, Å	23.711(2)	23.888(4)	23.843(1)	22.150(6)	10.0661(7)
b, Å	23.470(3)	23.746(4)	23.6914(11)	16.423(4)	10.2335(7)
c, Å	21.496(2)	21.433(4)	21.3451(9)	19.316(5)	17.7113(13)
α, °	90	90	90	90	82.2490(10)
β, °	109.243(5)	108.830(2)	108.757(2)	106.648(4)	78.7020(10)
γ, °	90	90	90	90	82.3580(10)
V, Å ³	11294(2)	11506(4)	11416.9(9)	6732(3)	1762.1(2)
ρ, mg m ⁻³	1.292	1.319	1.432	1.388	1.472
Abs. coeff., mm ⁻¹	1.182	1.190	5.096	1.211	1.736
F(000)	4608	4752	5008	2880	800.0
Crystal size, mm	0.27 x 0.25 x 0.22	0.37 x 0.35 x 0.35	0.18 x 0.09 x 0.07	0.36 x 0.20 x 0.10	0.27 x 0.18 x 0.16
θ range, °	2.47 to 29.999	1.244 to 27.500	3.06 to 68.24	1.568 to 27.495	1.18 to 27.53
Reflns collected	16464	51795	22960	59304	23339
Ind. reflns	14694	13208	10174	15435	8055
R(int)	0.0375	0.0188	0.0363	0.0347	0.0200
Obs. reflns [I > 2σ(I)]	58947	12117	8780	12833	7274
Completeness to 2θ	99.8%	100%	97.2%	100%	99.4%
Goodness-of-fit F ²	1.052	1.031	1.062	1.021	1.808
Final R [I > 2σ(I)]	R1 = 0.0228 wR2 = 0.0617	R1 = 0.0199 wR2 = 0.0529	R1 = 0.0344 wR2 = 0.0881	R1 = 0.0257 wR2 = 0.0581	R1 = 0.0404 wR2 = 0.1220
R (all data)	R1 = 0.0269 wR2 = 0.0636	R1 = 0.0225 wR2 = 0.0543	R1 = 0.0409 wR2 = 0.0919	R1 = 0.0358 wR2 = 0.0628	R1 = 0.0448 wR2 = 0.1261

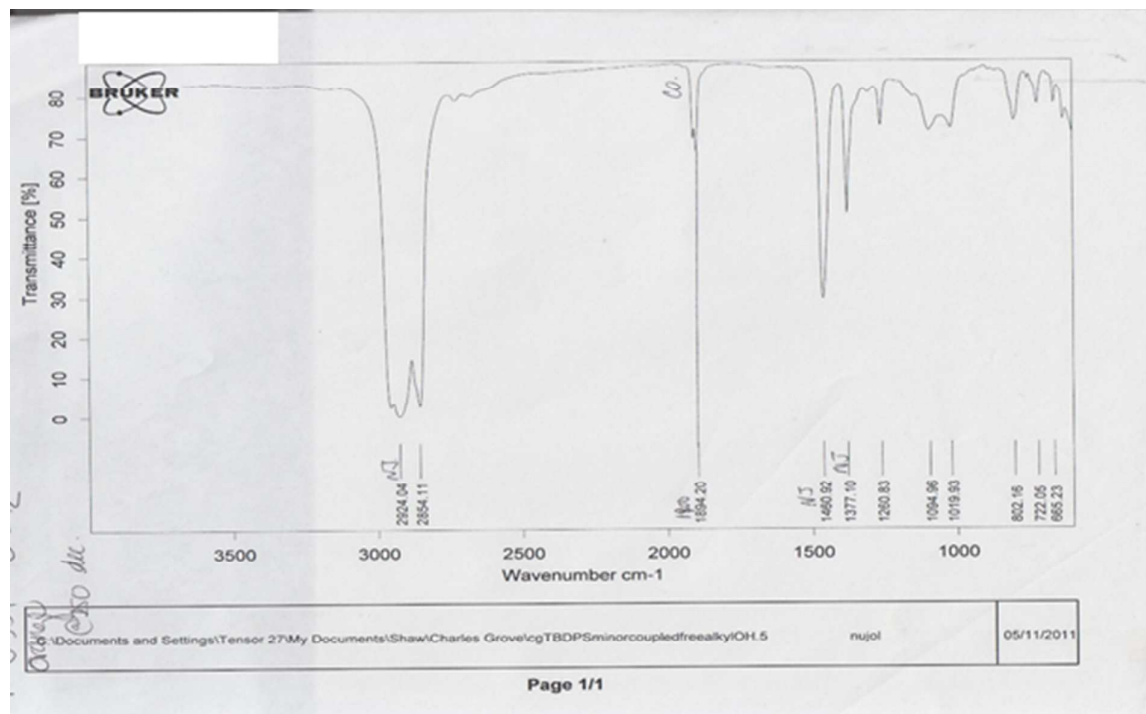


Figure S1: IR spectrum for *trans*-[Cr(GaArⁱPr₄)₂(CO)₄] (**1**) Nujol Mull

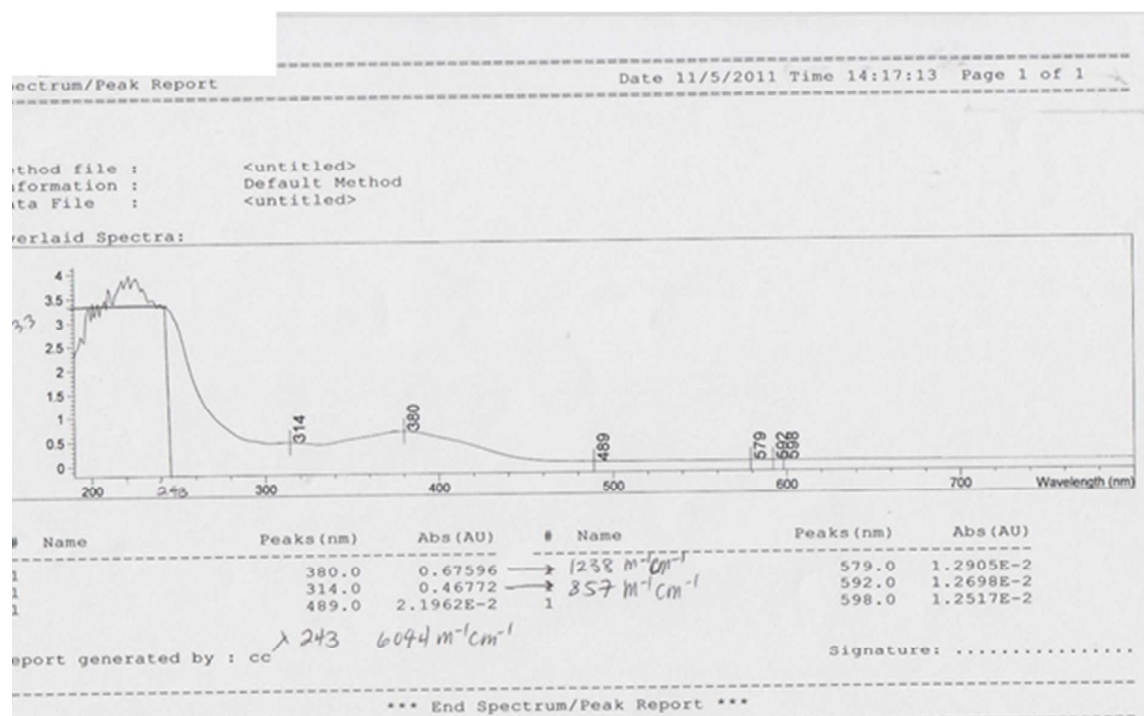


Figure S2: UV-Vis spectrum for *trans*-[Cr(GaArⁱPr₄)₂(CO)₄] (**1**) in hexanes at 25°C

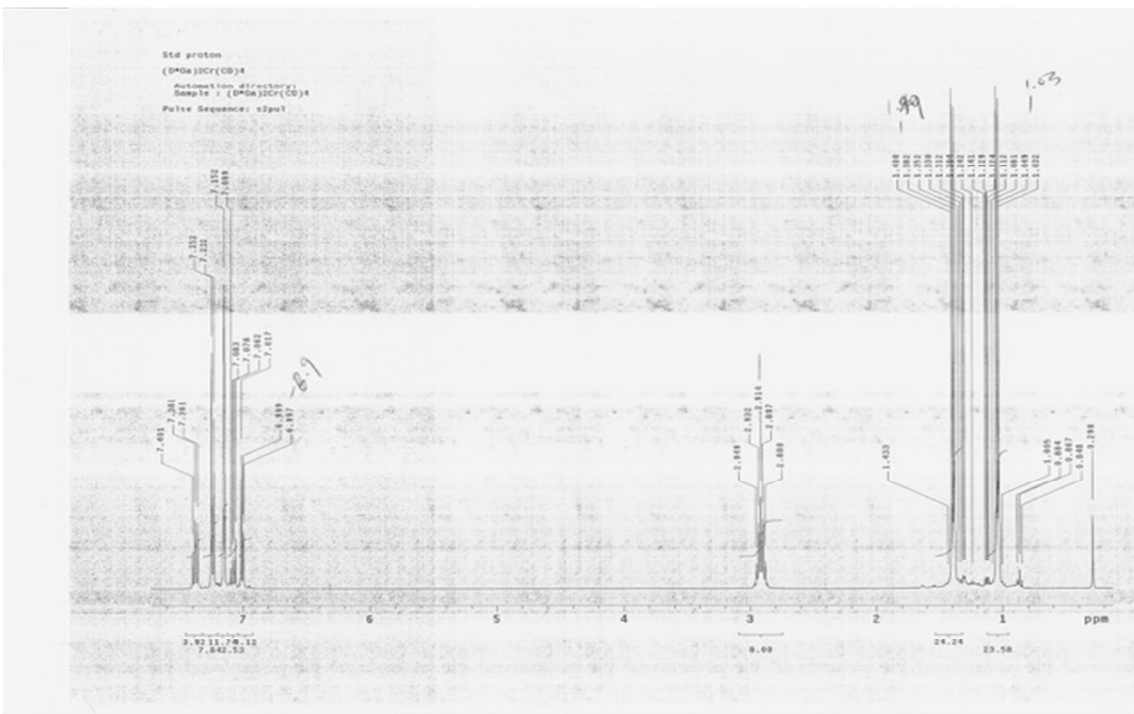


Figure S3: ^1H NMR spectrum for *trans*-[Cr(GaAr $i\text{Pr}_4$) $_2$ (CO) $_4$] (**1**) in C_6D_6 at 25°C

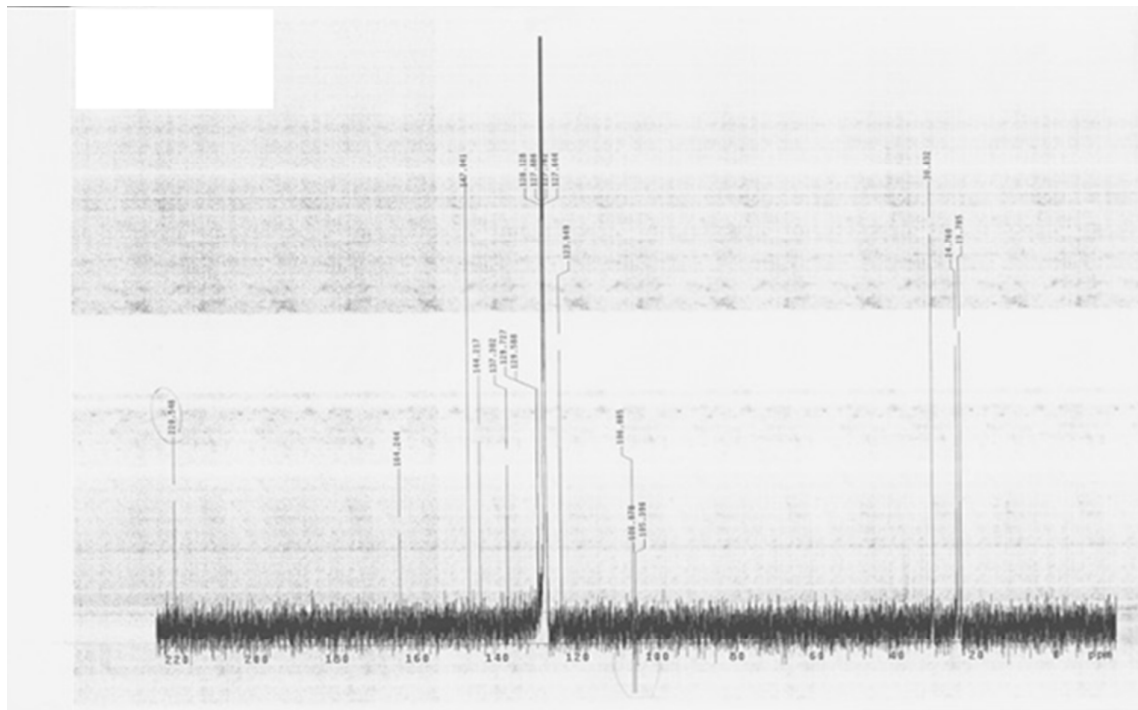


Figure S4: $^{13}\text{C}\{\text{H}\}$ spectrum for *trans*-[Cr(GaAr $^i\text{Pr}_4$) $_2$ (CO) $_4$] (**1**) in C $_6$ D $_6$ at 25°C

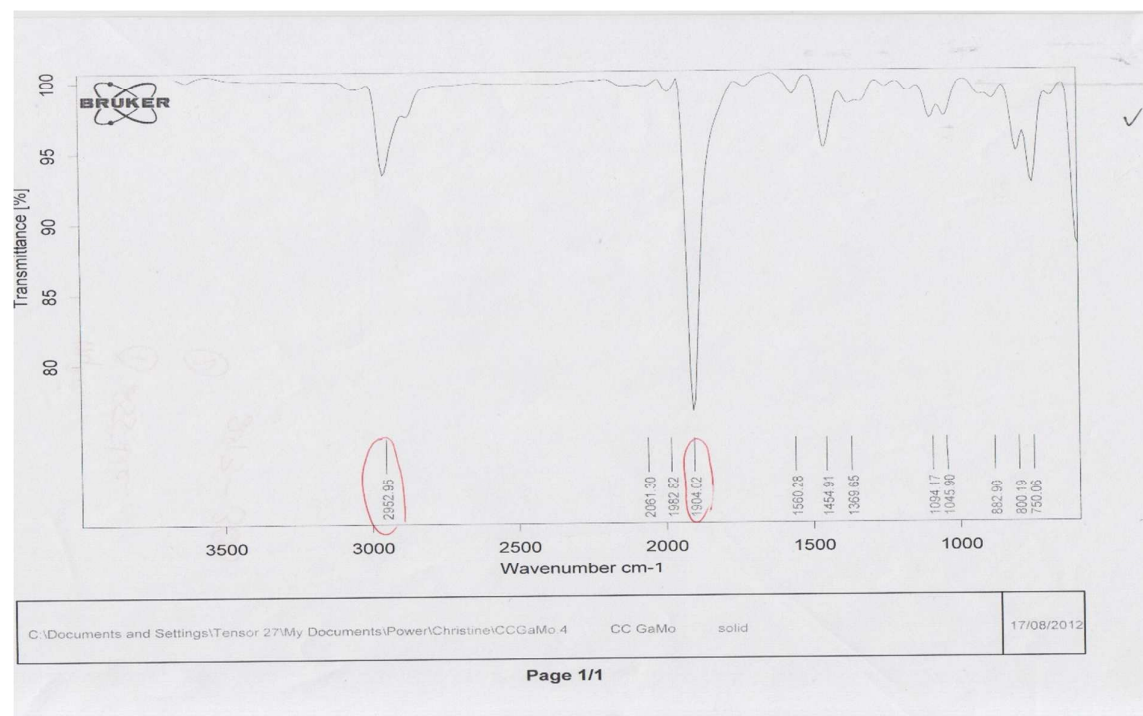


Figure S5: IR spectrum for *trans*-[Mo(GaAr $^i\text{Pr}_4$) $_2$ (CO) $_4$] (**2**)

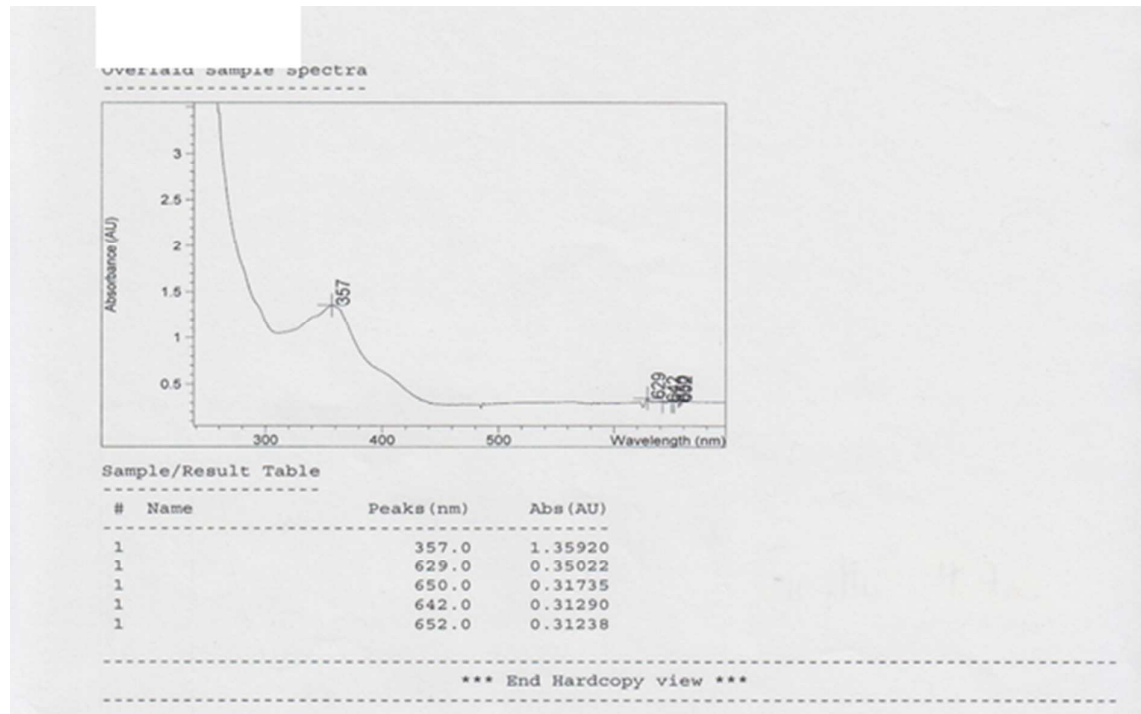


Figure S6: Electronic spectrum for *trans*-[Mo(GaArⁱPr₄)₂(CO)₄] (**2**)

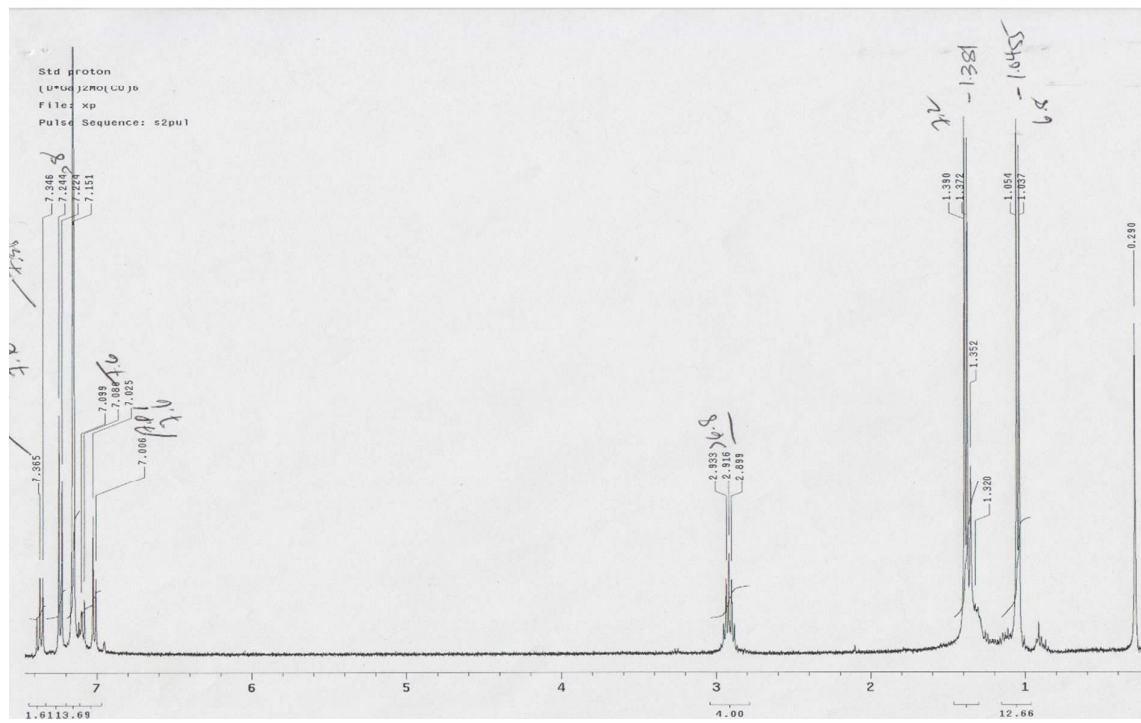


Figure S7: ^1H NMR spectrum for *trans*-[Mo(GaAr $^{i\text{Pr}_4}$)₂(CO)₄] (**2**) in C₆D₆ at 25°C

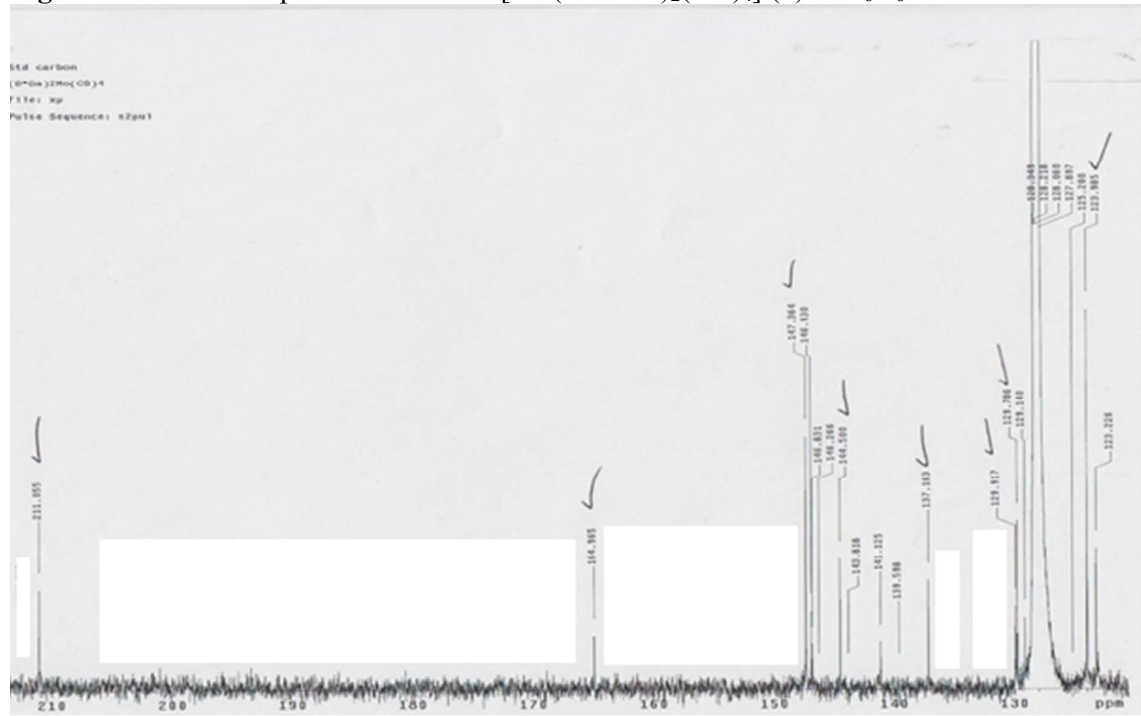


Figure S8: $^{13}\text{C}\{^1\text{H}\}$ spectrum for *trans*-[Mo(GaAr $^{i\text{Pr}_4}$)₂(CO)₄] (**2**) in C₆D₆ at 25°C

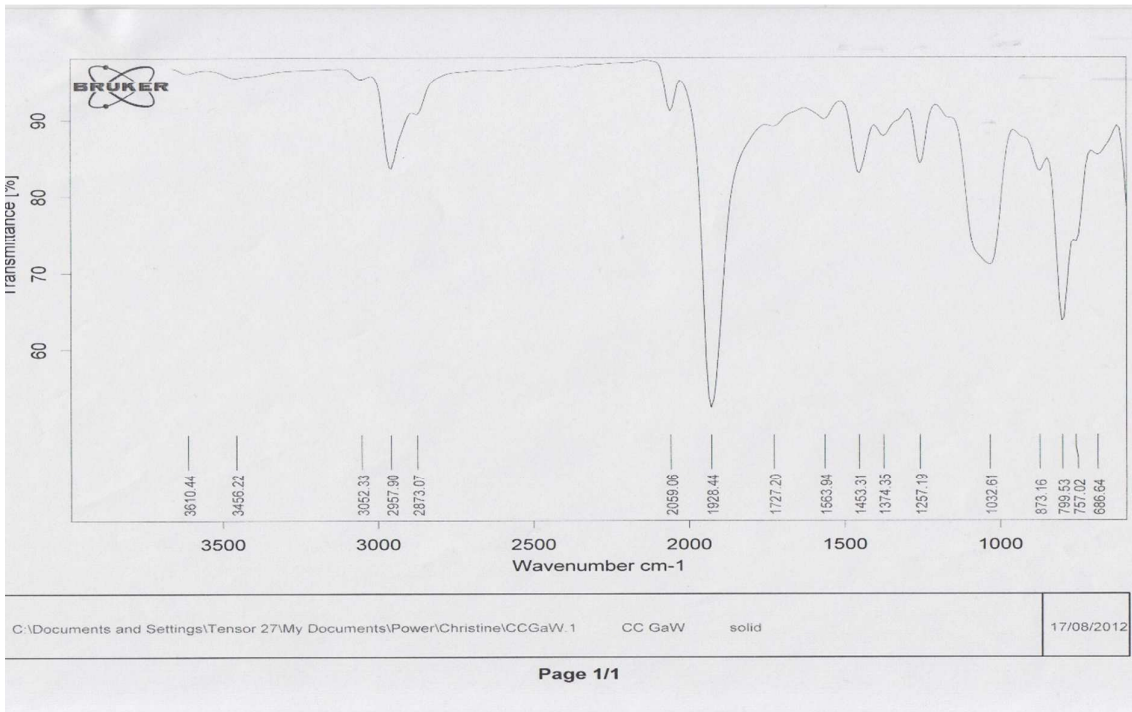


Figure S9: IR spectrum for *trans*-[W(GaArⁱPr₄)₂(CO)₄] (**3**) Nujol Mull

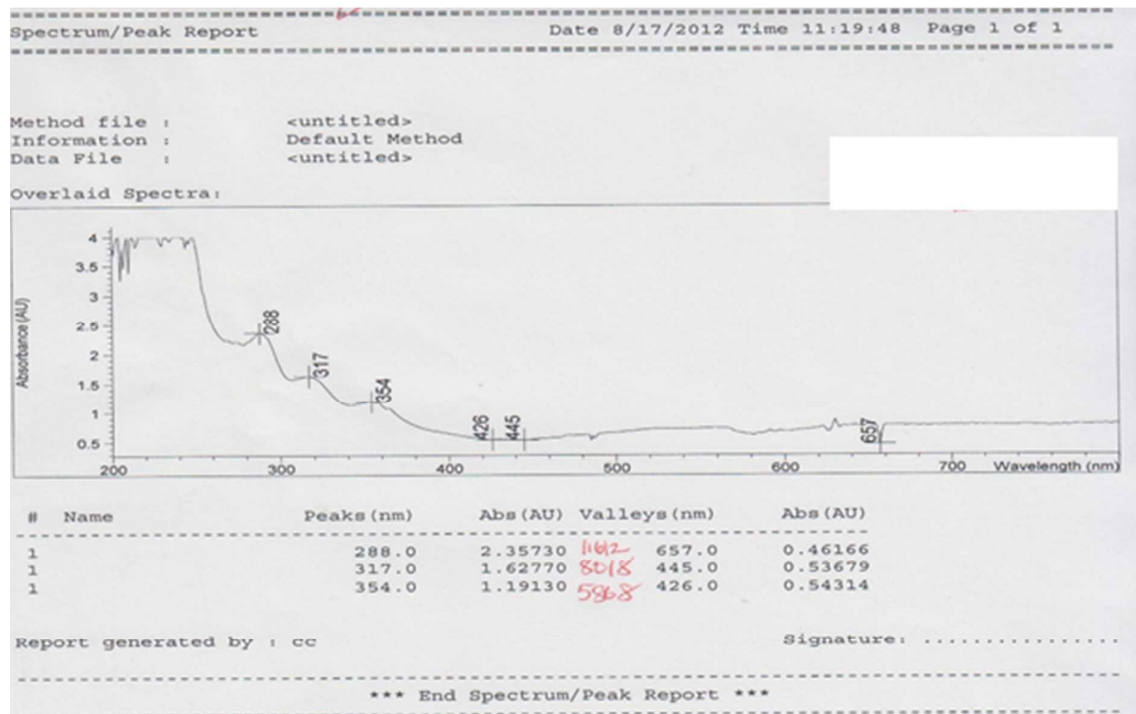


Figure S10: Electronic spectrum for *trans*-[W(GaArⁱPr₄)₂(CO)₄] (**3**) in hexanes at 25°C



Figure S11: ^1H NMR spectrum for *trans*-[W(GaArⁱPr₄)₂(CO)₄] (**3**) in C₆D₆ at 25°C

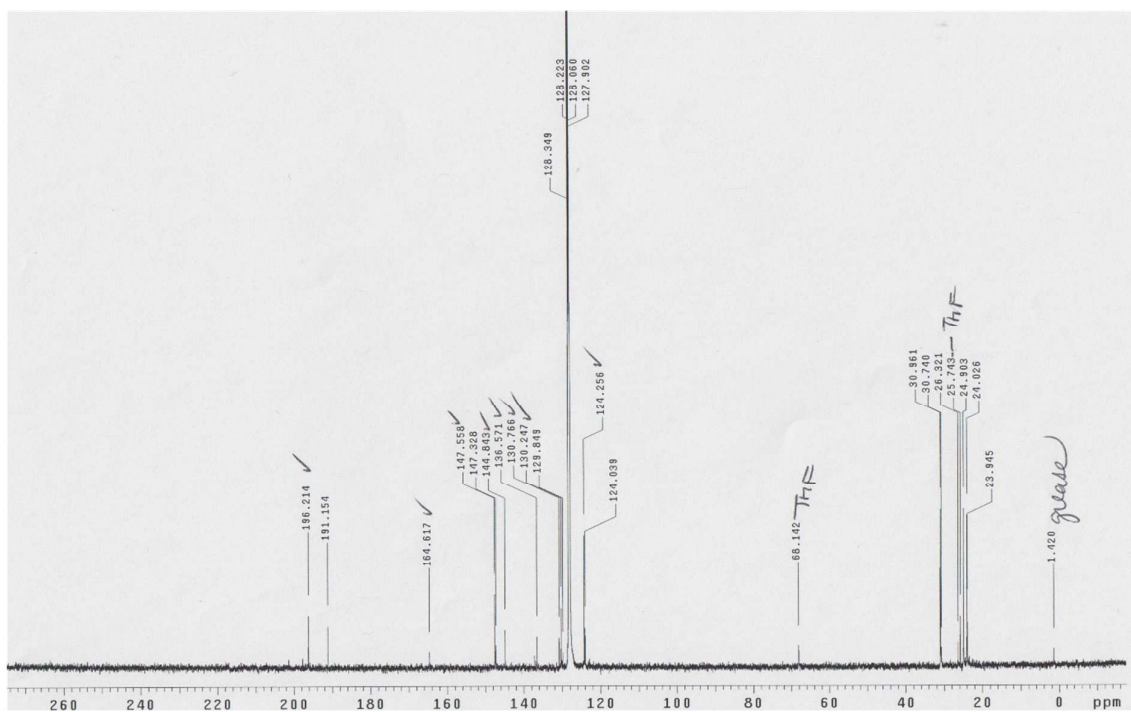


Figure S12: $^{13}\text{C}\{^1\text{H}\}$ spectrum for *trans*-[W(GaArⁱPr₄)₂(CO)₄] (**3**) in C₆D₆ at 25°C

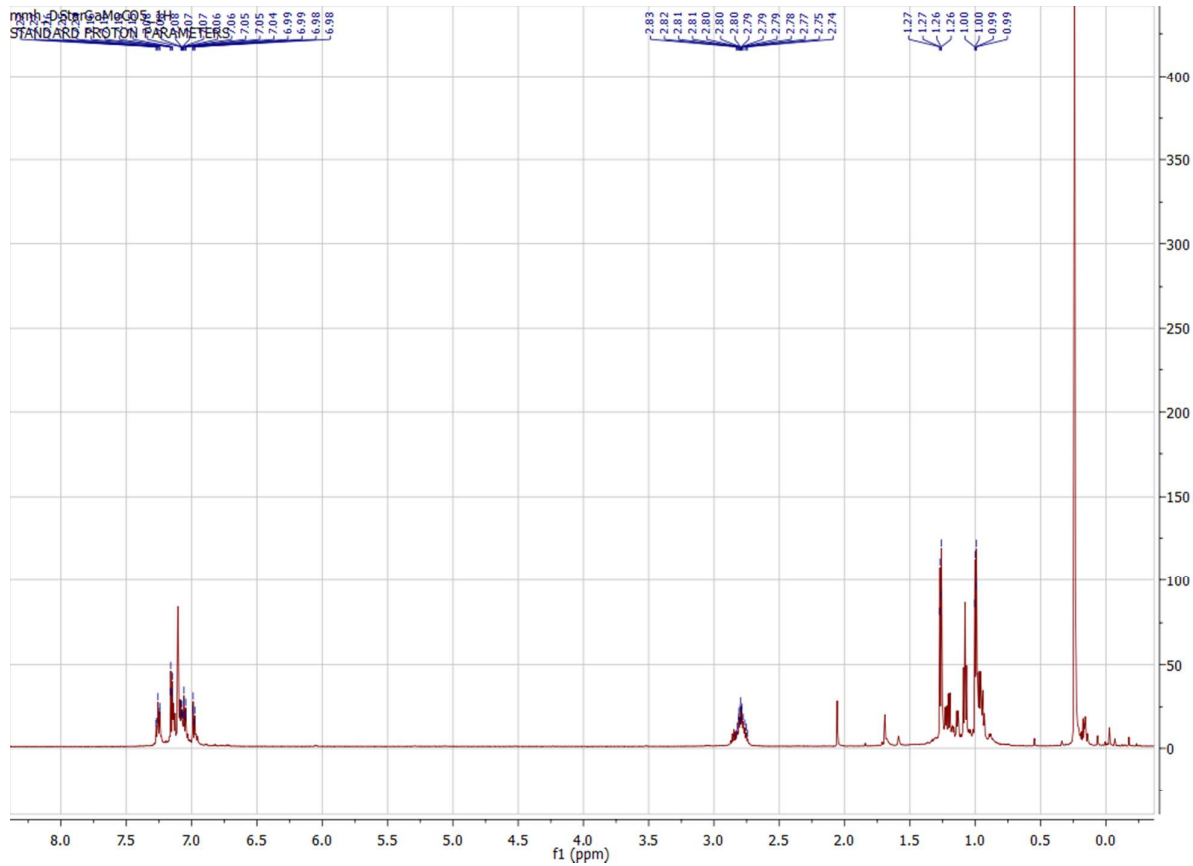


Figure S13: ¹H NMR spectrum for [Mo(GaAr*i*Pr₄)(CO)₅] (**4**) in C₆D₆ at 25°C

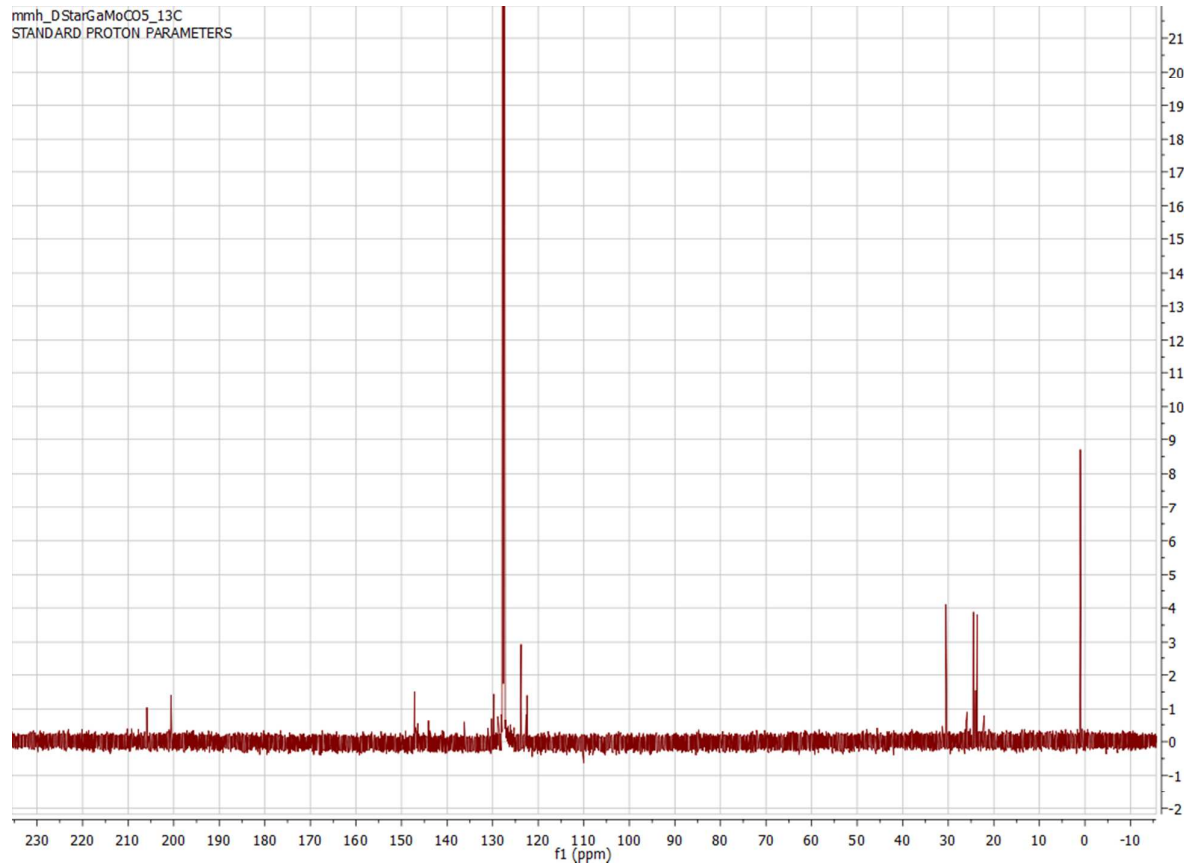


Figure S14: $^{13}\text{C}\{^1\text{H}\}$ spectrum for $[\text{Mo}(\text{GaAr}^{i\text{Pr}_4})(\text{CO})_5]$ (**4**) in C_6D_6 at 25°C

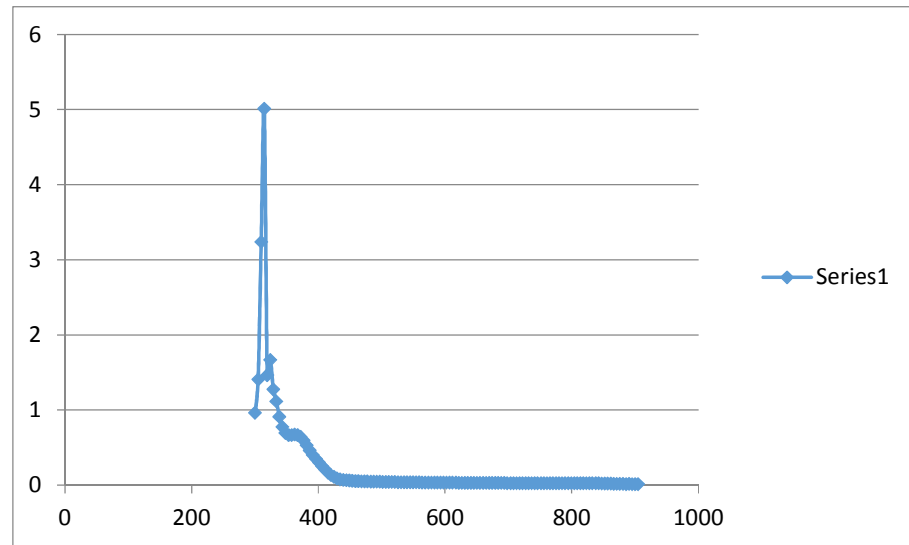


Figure S15: Electronic spectrum for $\text{Mo}(\text{GaAr}^{i\text{Pr}_4})(\text{CO})_5$ (**4**) in hexanes at 25°C

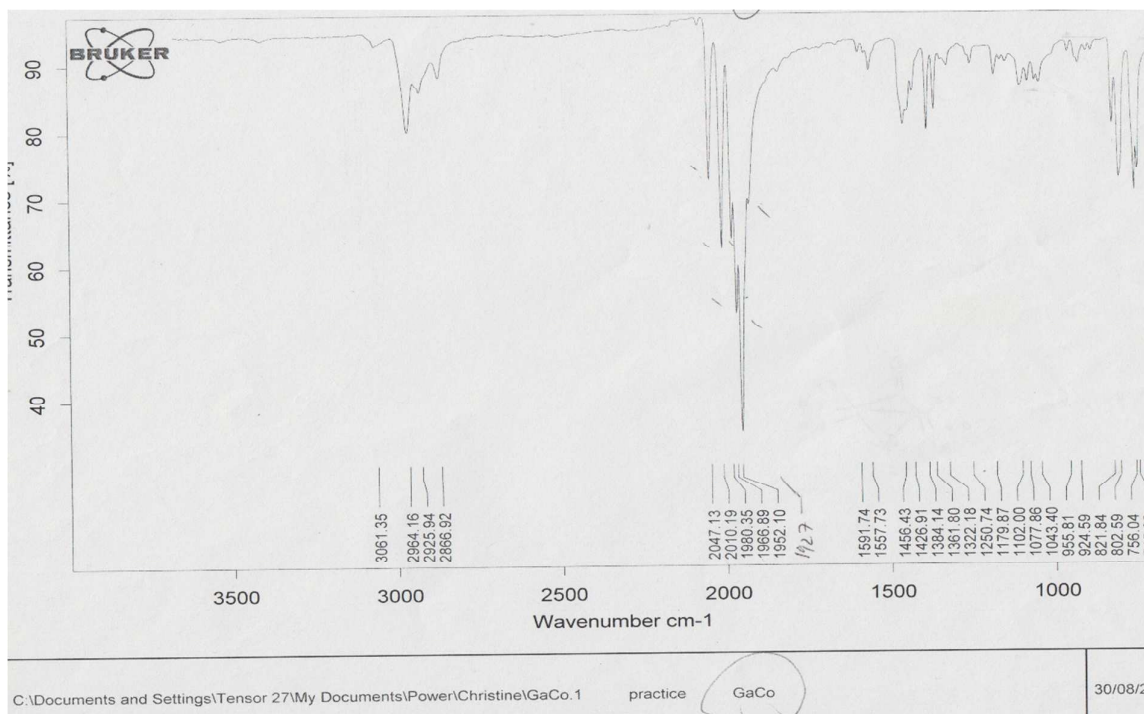


Figure S16: IR spectrum for $\text{Co}_2(\mu\text{-GaAr}^{\text{Pr}4})(\mu\text{-CO})(\text{CO})_6$ (**5**) Nujol Mull

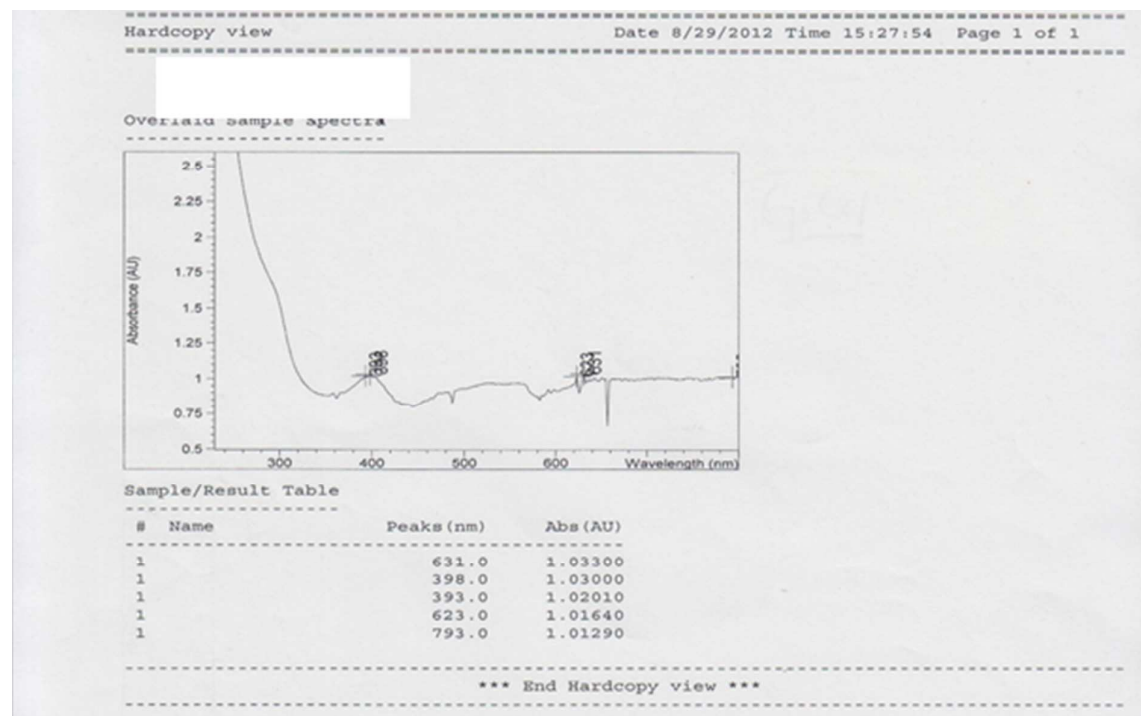


Figure S17: Electronic spectrum for $\text{Co}_2(\mu\text{-GaAr}^{\text{Pr}4})(\mu\text{-CO})(\text{CO})_6$ (**5**) in hexanes at 25°C

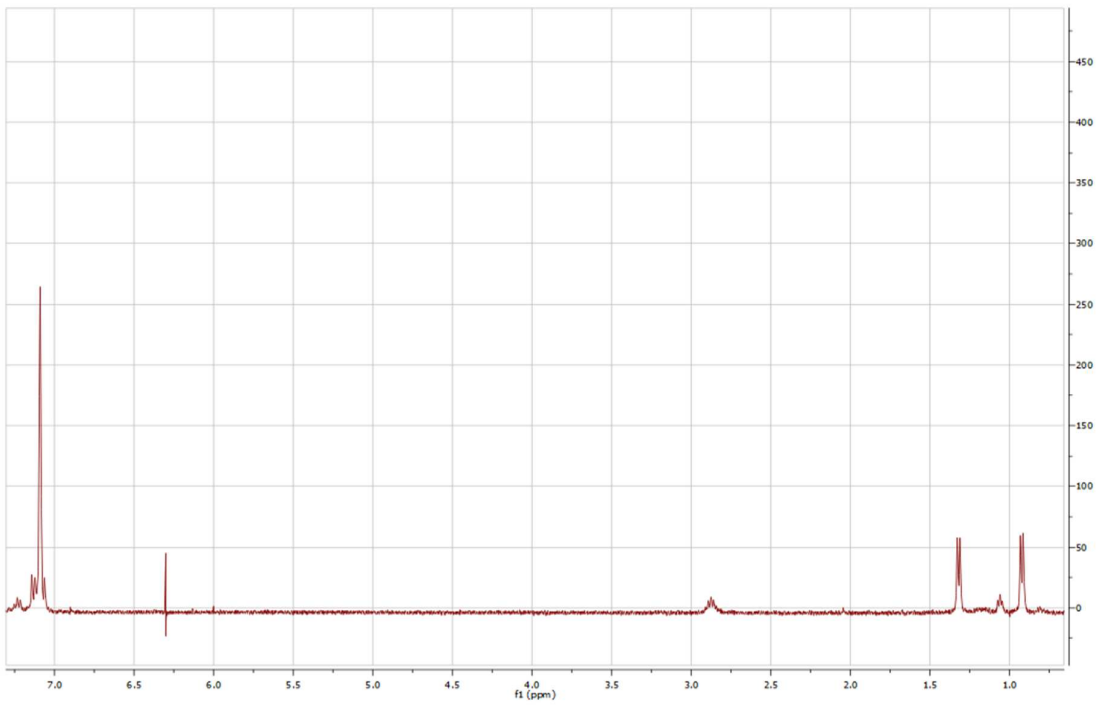


Figure S18: ^1H NMR spectrum for $\text{Co}_2(\mu\text{-GaAr}^{i\text{Pr}_4})(\mu\text{-CO})(\text{CO})_6$ (**5**) in C_6D_6 at 25°C

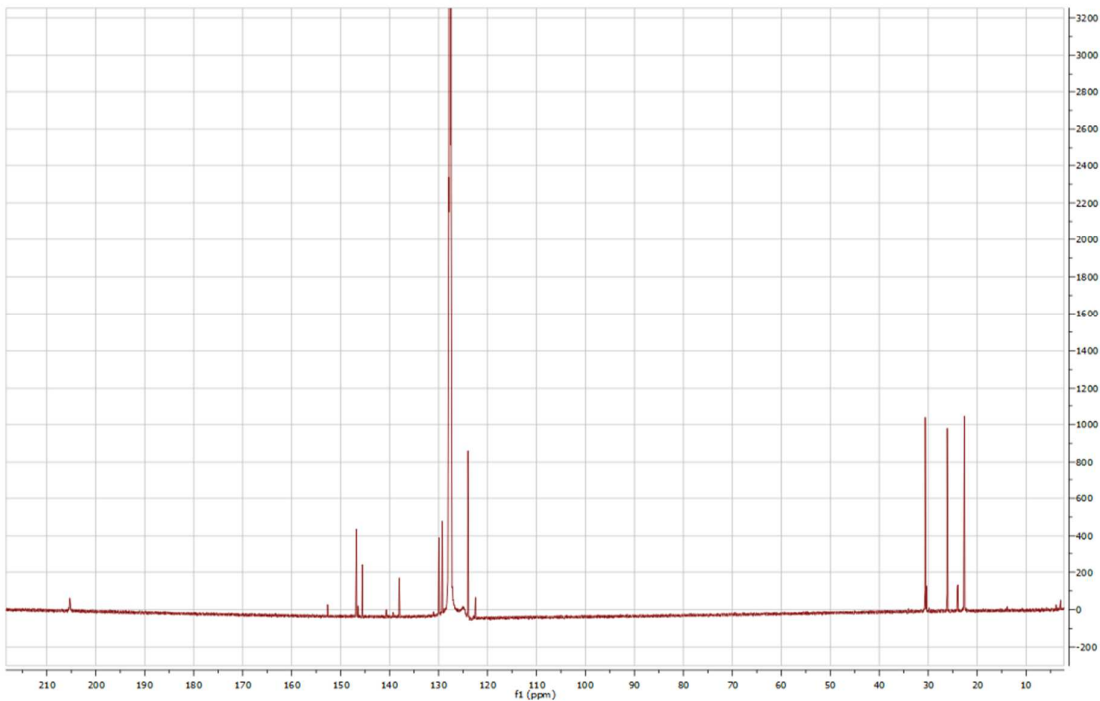


Figure S19: $^{13}\text{C}\{^1\text{H}\}$ spectrum for $\text{Co}_2(\mu\text{-GaAr}^{i\text{Pr}_4})(\mu\text{-CO})(\text{CO})_6$ (**5**) in C_6D_6 at 25°C